

How much water can bioretention retain, and where does it go?

Sylvie Spraakman^a, Jean-Luc Martel^b and Jennifer Drake^{a,*}

^a Department of Civil and Mineral Engineering, University of Toronto, 35 St. George Street, Toronto, ON M5S 1A4, Canada

^b Hydrology and Climate Change Laboratory, École de technologie supérieure, 1100 Notre-Dame West Street, Montreal, QC H3C 1K3, Canada

*Corresponding author. E-mail: jenn.drake@utoronto.ca

 JD, 0000-0001-6235-3918

ABSTRACT

Bioretention is a type of green stormwater infrastructure for the urban environment that mimics a natural hydrologic system by reducing peak flows and runoff volumes and encouraging infiltration and evapotranspiration. This study examines the complete water balance of a bioretention system located in Vaughan, Ontario, Canada, between 2018 and 2019. The water balance was further broken down by event size, where the event size was determined by rainfall frequency analysis. Recharge was the largest component of the water balance overall (88% of inflow), as well as by event size. Evapotranspiration was the next largest water balance component (6% of inflow overall), and was a significant component of inflow (19%) when considering only small events (50% probability of recurrence). Evapotranspiration is a slow but consistent process, averaging 2.3 mm/day overall and 2.9 mm/day during the growing season. Climate change is likely to bring more wet days and higher temperatures, which will impact the bioretention water balance by increasing evapotranspiration and inflow. Design standards for retention targets should be updated based on the most recent rainfall frequency analyses to adjust for changing climate conditions.

Key words: evapotranspiration, infiltration, low impact development, rain gardens, stormwater, water balance

HIGHLIGHTS

- Evapotranspiration (ET) is a significant component of the water balance.
- 19% of inflows were released as ET when considering only small events.
- ET is a slow but consistent process.
- Ignoring ET may lead to oversizing of green infrastructure systems.
- Design standards for retention targets should be updated based on recent rainfall frequency analysis.

INTRODUCTION

Degraded water quality in lakes and streams has been a focus of engineers and scientists in recent decades, leading to solutions to reduce industrial, wastewater treatment plant and agricultural discharges. Stormwater runoff is a non-point source of pollution to water bodies, and so requires a more distributed approach to treatment. Stormwater runoff in highly impervious areas contains a multitude of contaminants that are harmful to water quality and aquatic life (Marsalek *et al.* 1999). Peak flows and increased runoff volumes also have impacts on erosion and sedimentation in urban streams which further degrade aquatic environments (Walsh *et al.* 2005). Broadly, green infrastructure is defined as any system that uses plants, soil, permeable surfaces or substrates, water harvesting or re-use or landscaping to promote the natural hydrologic cycle in urban environments, including increasing the amount of water returned to the environment via infiltration and evapotranspiration and reducing the amount of overland runoff (US EPA 2020). The overall theory behind the green stormwater infrastructure (GSI) is that by retaining the water closer to the source where it falls and reducing the peak and volume of runoff, less sediment and fewer pollutants will make it to our streams, thereby improving water quality, reducing erosion and increasing recharge to groundwater (US EPA 2020).

The design of the GSI is focused on optimizing the retention of stormwater runoff. The GSI is primarily designed for the more frequent rainfall conditions of a local environment. In the northeastern United States, where the GSI has been heavily researched (Spraakman *et al.* 2020a), a 25-mm rainfall event has become the standard design storm (Maryland Department of the Environment 2009). This typically represents the 90th

This is an Open Access article distributed under the terms of the Creative Commons Attribution Licence (CC BY 4.0), which permits copying, adaptation and redistribution, provided the original work is properly cited (<http://creativecommons.org/licenses/by/4.0/>).

percentile of all rainfall events in the northeastern United States, meaning that 90% of events are less than 25 mm, based on past rainfall patterns. In designing stormwater management systems, engineers often model at an event-scale, using events larger than the 90th percentile depth or using design storms for 2- to 100-year return periods (also based on historical rainfall). Evapotranspiration is insignificant using this type of modelling due to the large storm volumes generated in these modelling exercises. Consider, for example, a 25-mm runoff event followed by 3 dry days at a site with a drainage area 10 times the size of the GSI. This 25-mm event would lead to approximately 250 mm of runoff entering the GSI. As evapotranspiration is a consistent and slow process, evapotranspiration might be 2–3 mm/day for the following 3 dry days, 6–9 mm in total or 2–4% of the inflow. During the largest runoff that a GSI is designed to retain, evapotranspiration is a very small component of the water balance and has often been overlooked by engineers and researchers.

However, the GSI and bioretention systems, in particular, are designed to retain events with a considerably higher frequency of occurrence. This necessitates reviewing the water balance at a more continuous scale. Despite the knowledge that bioretention systems are typically designed to retain the most frequently occurring rainfall events, all storm events are included in a typical water balance analysis. For example, past literature review compilations on bioretention systems have shown volume reductions between the large range of 50 and 95% (Davis *et al.* 2009; Liu *et al.* 2014), but these summaries account for all rainfall events in the study period, and no data are given on how many events actually met the retention target for which the bioretention system was designed.

Limited data are available on the whole water balance of bioretention systems, a type of GSI. The primary means of data collection for bioretention is measuring flow at the inlet, underdrain and overflow. For bioretention systems without an underdrain, all water that does not overflow is assumed to infiltrate or evapotranspire. Even though these are vegetated systems with soil media with water held between soil particles and within plants, evapotranspiration is rarely considered in the design. For example, Li *et al.* (2009) conducted a hydrologic study on a lined bioretention system with an underdrain, and it was assumed that the difference between the inlet and outlet volumes (19% reduction) was entirely attributed to evapotranspiration. Other studies estimated evapotranspiration via numerical models (*e.g.*, Penman–Monteith) (Muthanna *et al.* 2008; Selbig & Balster 2010; Strauch *et al.* 2015; Stewart *et al.* 2017), Morton (Bonneau *et al.* 2020) and Bowen Ratio Energy Balance (Sustainable Technologies Evaluation Program 2015), and found that evapotranspiration was between 2 and 25% of the influent runoff (the drainage area to the bioretention system area ratio varied from 8 to 25). Several bioretention lysimeter studies have been conducted (Denich & Bradford 2010; Wadzuk *et al.* 2015; Hess *et al.* 2017, 2019; Regehr 2019; Tirpak *et al.* 2019), with results showing estimated daily evapotranspiration values of 2–4 mm/day and a wide range of evapotranspiration as a portion of the inflow (10–60%).

Most studies of bioretention have focused on system hydrology (Sprakman *et al.* 2020a), though evapotranspiration has not been widely studied or accounted for beyond the studies listed above. Here we hypothesize that evapotranspiration is a significant portion of the water balance for events for which the GSI was designed to retain and that this has been previously missed due to the focus on water balance accounting that includes large events above the design retention value. This study focuses on rainfall events within the design criteria and rainfall statistics for the local area in which a bioretention system was installed. The research questions are as follows: (1) does the bioretention system retain the intended rainfall volume and (2) how is the water balance divided between infiltration, outflow and evapotranspiration? In this study, we determine the frequency of rainfall events to determine which events are large, medium and small events for this local area. The water balance data are then presented to show the retention amount and water balance by event size.

METHODOLOGY

Study site

The study site is a bioretention system located at the Kortright Centre for Conservation in Vaughan, Ontario, Canada (43° 49' 51.95" N 79° 35' 28.15" W), in the Koppen-Geiger climate zone Dfb, warm summer continental climate (Beck *et al.* 2018). The period of study was between August 21 to November 3, 2018, and May 1 to November 3, 2019. The bioretention system receives runoff from a parking lot and contains an underdrain. Complete physical characteristics of the bioretention system are summarized in Table 1, and a photo of the site is shown in Figure 1. The vegetation was chosen from the planting list provided by local guidelines (Credit Valley Conservation & Toronto & Region Conservation 2010), which are meant to be drought- and salt-tolerant

Table 1 | Physical characteristics of the bioretention system

Kortright Bioretention System	
Year constructed	2012
Drainage area (m ²)	265
Land use of drainage area	Impermeable parking lot made of rubber interlocking pavers
Bioretention area (m ²)	30
Drainage area to bioretention area ratio	9:1
Depth (m)	0.4
Media composition	Sand
Vegetation	Wildflowers, grasses and ground covers, including the following: <i>Rudbeckia hirta</i> , <i>Echinacea purpurea</i> , <i>Panicum virgatum</i> , <i>Eupatorium purpureum</i>
Underdrain	10-cm diameter perforated pipe inside 15-cm deep clearstone layer Restricted orifice on underdrain pipe: valve at 80% closed
Underlying soils	Silty clay

**Figure 1** | Bioretention system in July 2018, including all monitoring equipment.

species due to salt applied to parking lots and roadways in the winter in this climate. This system was constructed in an existing green space area for the purpose of research, and was not designed for the retention of a particular rainfall event. Based on its sizing, it should be able to retain the 15-mm event for this drainage area (see [Table 1](#)).

Rainfall statistics

Rainfall data between the months of May and November for the years 2008–2020 were available for Toronto and Region Conservation Authority station HY039, located approximately 500 m from the studied bioretention system. Rainfall data were recorded every 5 min with an accuracy of $\pm 2\%$ with a tipping bucket (TB3 0.2 mm, Hydrological Services, Lake Worth, FL, USA). The HY039 weather station also had a soil moisture sensor (S-SMC-M003, Onset Computer Corporation, Bourne, MA, USA), which measured volumetric water content at 25 cm beneath the soil surface in the surrounding fallow field. This data were made available using the Toronto and Region Conservation Authority Open Data License ([Toronto & Region Conservation Authority 2020](#)).

Rainfall events were extracted from the HY039 rain gauge using the storm event detection (SED) method suggested by Leimgruber *et al.* (2018). The main steps of the SED method are schematized in Figure 2. The four parameters necessary for extracting the rainfall events are based on typical values:

- *Threshold time*: 60 min – The period of time during which the threshold value must be exceeded.
- *Threshold value*: 1 mm – The threshold value to be considered as a rainfall event.
- *Inter-event duration*: 360 min – The minimum gap defining two separate rainfall events.
- *Time extension*: 60 min – Extension of the period after the end of the event to be included in the event.

Using this methodology, all available rainfall events respecting the above parameters were extracted and used to define local rainfall statistics to better assess the performance of the bioretention system.

Water balance measurement

A range of instruments was used to estimate the complete water balance in the bioretention system. Rainfall from the HY039 station was used to estimate inflow to the system. Flow at the bioretention outlet was measured at the underdrain, and evapotranspiration was measured with a lysimeter. The measurement method, calculation, and uncertainty are described below. For consistency, all terms in the water balance are expressed in units of depth (millimetres), with the depth relative to the area of the bioretention system.

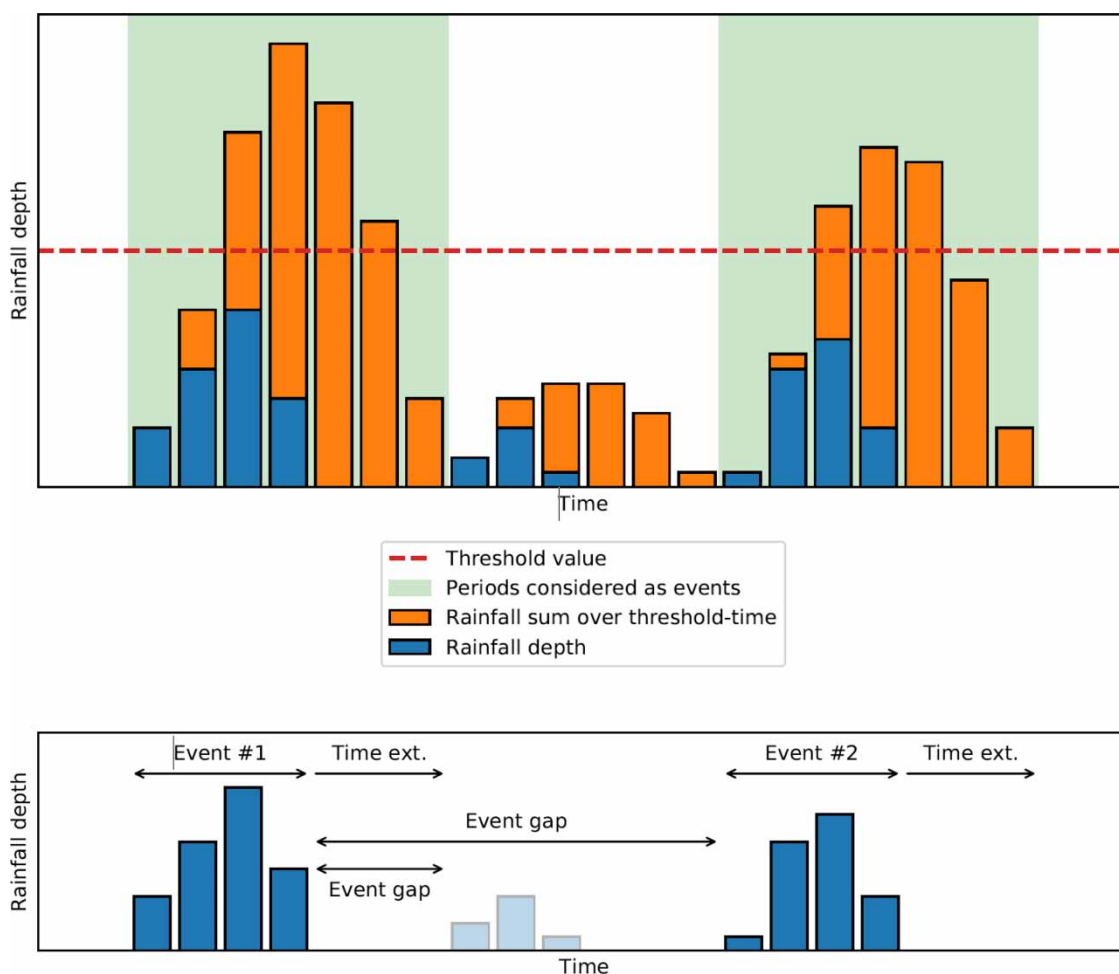


Figure 2 | Schematization of the SED method and the main parameters defining events. The middle-event is excluded for being below the precipitation threshold. Adapted from Leimgruber *et al.* (2018).

Inflow

The rainfall data from HY039 were considered as the best estimation of the inflow in the bioretention system. The inflow for the bioretention system is calculated as:

$$I \text{ (mm)} = P \text{ (mm)} \times 0.95 \times 9 \quad (1)$$

where I is the inflow at the bioretention system in mm, P is the precipitation (rainfall) in mm, 0.95 is the runoff coefficient for an impermeable parking lot (Chin 2013b), and 9 is the ratio of the total drainage area to the bioretention area (see Table 1).

Underdrain flow

The only outlet for this bioretention system was a perforated underdrain pipe. The system was not designed with an overflow, and stormwater will back up into the parking lot if the system's capacity is exceeded. The pipe was non-perforated at its exit from the bioretention system. The flow in the underdrain was partially throttled using a valve at approximately 80% closed located at a nearby monitoring hut to limit the flow rate leaving the bioretention and encourage infiltration. The monitoring hut contained a 3-l tipping bucket with an accuracy of $\pm 2\%$ (V2A Tipping Counter, Geneq Inc, Montreal QC). The volume of outlet flow was calculated by multiplying the number of tips by 3 l and then converted to depth units by dividing by the bioretention area.

$$O \text{ (mm)} = \frac{0.003 \text{ m}^3 \times \text{count}}{\text{Bioretention area (m}^2\text{)}} \times \frac{1000 \text{ mm}}{\text{m}} \quad (2)$$

Retention and reduction

The amount of water retained in the bioretention system was calculated as the difference between inflow and outflow. Retention does not differentiate between evapotranspiration and recharge. The volumetric reduction was calculated as the retention divided by the inflow. Equations for retention and reduction are shown in the following.

$$\text{Retention (mm)} = I \text{ (mm)} - O \text{ (mm)} \quad (3)$$

$$\text{Volume Reduction (\%)} = \frac{I \text{ (mm)} - O \text{ (mm)}}{I \text{ (mm)}} \times 100 \quad (4)$$

Lysimeter

A Smart Field Lysimeter (30 cm tank height, UMS, Munich, Germany) was installed in the bioretention system in summer 2017. Due to a malfunctioning pump system which was replaced, only the data following August 21, 2018, were considered. The system remained in place inside the bioretention system during the winter months, but these data were not considered in the water balance analysis. The daily evapotranspiration dataset is available to download via HydroShare (Sprakman & Drake 2021).

The lysimeter consisted of a tank of bioretention soil cut from a core within the existing bioretention system, sitting on top of a scale measuring the mass every minute. The lysimeter was placed in the middle of the bioretention system and was partially shaded by a large existing tree located immediately west of the bioretention system. The tank was planted with *Rudbeckia hirta*, which was transplanted from elsewhere in the system. *Rudbeckia hirta* was selected as the plant in this study because of its prominence in this system and a perception by the authors that it was a popular plant in stormwater plantings. This enclosed tank was connected to a water tank, which drained water from the lysimeter when the lysimeter was saturated and added water to the lysimeter during dry periods, automatically using the difference in tension between the lysimeter tensiometer and a tensiometer located within the undisturbed bioretention soil. The lysimeter tank also contained sensors for matrix potential (MPS2, UMS, Munich, Germany) and volumetric water content (5TE, UMS, Munich, Germany).

The mass data from the lysimeter were used to determine the evapotranspiration. The mass data were post-processed using the methodology and programming outlined in Hannes *et al.* (2015), using all of the standard filter parameters except for the oscillation threshold of 10 g to minimize errors. Even with appropriate post-processing of the mass data it is conservative to assume that evapotranspiration fluxes may have an overall error of $\pm 10\%$

(Hannes *et al.* 2015). The fluxes in lysimeter mass and evapotranspiration (E) were calculated as follows:

$$J(t_i) = \frac{M_{i+1} - M_i}{t_{i+1} - t_i} \quad (5)$$

$$\text{If } J(t_i) < 0, \text{ then } E(t_i) = -J(t_i), \text{ else } E(t_i) = 0 \quad (6)$$

where J is the lysimeter mass flux, M is the total mass of the lysimeter system, t is the time, i is the time step, and E is evapotranspiration. Since the surface area of the lysimeter is 0.0707 m^2 , the lysimeter mass flux (J) was multiplied by 14.15 mm/kg to obtain water depth (UMS gmbH Munchen 2014).

Volumetric water content (VWC , m^3/m^3) sensors were used to calculate the change in storage within the lysimeter. The sensors were located at three depths (top 0–10 cm, middle 10–20 cm, and bottom 20–30 cm) in the lysimeter column, and so the average of the three sensors was taken. The storage and change in storage (S) were calculated as follows:

$$S = \frac{VWC_1 + VWC_2 + VWC_3}{3} \times \text{tank height (mm)} \quad (7)$$

$$\Delta S(t_i) = \frac{S_{i+1} - S_i}{t_{i+1} - t_i} \quad (8)$$

Water balance calculations

The full water balance calculation was completed using measurements from the instruments described above. The full water balance is captured using this equation:

$$R \pm \varepsilon = P + I - O - E - \Delta S \quad (9)$$

where R is the groundwater recharge (mm), ε is the residuals or error (mm), P is the precipitation (mm) falling on the bioretention system directly, I is the inflow (mm), O is the outflow (mm), E is the evapotranspiration (mm), and ΔS is the change in storage (mm).

Recharge and residuals are the unknowns in the above equation. Recharge represents the amount of water that exits the bioretention system through the bottom of the system and sidewall areas and enters the shallow groundwater system. The residuals represent errors in the system, primarily due to the variety of different instruments, as well as remaining water in the bioretention system, which is not measured at the lysimeter. Each measured parameter (change in storage, inflow, outflow, and evapotranspiration) has a degree of error or uncertainty. Tipping buckets (for inflow and outflow) have an accuracy of $\pm 2\%$, and the lysimeter scale has an accuracy of $\pm 0.1 \text{ g}$, which is less than 1% of the system's total mass. Due to the low error in the system, residuals are ignored, and recharge to groundwater was then calculated directly from the other variables. Overflow is not included in the water balance (Equation (9)). This system was designed in a retrofit scenario and did not have a designed overflow structure. If stormwater runoff exceeds the system's capacity, the water will back up into the parking lot. This was observed only once in 2013, shortly after initial construction, during a very large rain event (July 8, 2013, 139 mm of rainfall over 8 h). Overflow, where the stormwater backed up into the parking lot, has not been observed since then and not during the monitoring period of this study.

To analyze the water balance, all variables were summed over a period considered as an event, which was split into three categories based on the frequency of the rainfall events: small (<50% probability density), medium (between 50 and 80% probability density) and large-sized events (>80% probability density). Each water balance event was composed of a 1-day wet event (corresponding to the rainfall event day of occurrence) and the following dry period, referred to herein as a dry event, if applicable. For instance, two days with more than 1-mm of rainfall followed a dry period of 3 days would correspond to two water balance events: (1) one wet event (1-day duration) and (2) one wet event followed by a dry event (4-day duration). The water balance components for water leaving the system (evapotranspiration, recharge, and outflow) are shown as a portion of the components adding water to the system, or inflow, via the inflow from the parking lot runoff and precipitation falling on the system.

The time step used for the water balance was daily. Rainfall events all had varying durations, with the longest duration being 17 h. The lysimeter, rain gauge, and outlet tipping bucket all used different reporting periods for the raw data (either 1 or 5 min), so reconciling the raw data would need summarizing at either hourly or daily levels. As evapotranspiration and recharge are both slow processes, a daily time step was chosen. The water balance equation is represented visually in Figure 3. The table of wet events and corresponding data fields (duration, intensity, daily inflow, outflow, recharge, and evapotranspiration) is provided in the Supplementary Material.

The Shapiro–Wilks test for normality found that the distribution of recharge, evapotranspiration and outflow did not follow normal distribution at the 5% significance level. The difference between the water balance parameters for the three event-size categories (small, medium, and large, as described above) were tested for statistical significance using the Kruskal–Wallis H -test (the non-parametric equivalent of the ANOVA test) (Corder & Foreman 2009). All calculations and statistics were performed in python using pandas (McKinney & Pandas Development Team 2021), NumPy (Harris *et al.* 2020), Matplotlib (Hunter 2007), and SciPy (Virtanen *et al.* 2020) libraries.

RESULTS

Rainfall statistics

There were 466 rainfall events measured at HY039 during May–November 2018–2020 that were extracted using the methodology described previously (see Figure 2). The cumulative distribution function (CDF) curve for all events shown in Figure 4 indicates that 50, 80, and 90% of rainfall events were respectively less than or equal to a total depth of 5.4, 15.2, and 21.8 mm. For this study, events with a 50% probability density are small events (<5.4 mm), events between 50 and 80% probability density are medium events (between 5.4 and 15.2 mm), and large events are those with an 80% probability density (>15.2 mm).

Inlet and outlet flow, reduction, and retention

The average volume reduction across all events during this monitoring period was 97%, and the average retention was 31.2 mm/day. Inflow ranged from 0.7 to 187 mm/day (recall this is nine times larger than precipitation from Equation (1)), and outflow ranged from 0 to 43 mm/day. The average inlet and outlet flows and retention during this monitoring period are shown in Table 2, and the CDFs for inflow and outflow are shown in Figure 5. The largest outflows were recorded during August 2018, though note that this average only covers August 21–31, 2018, whereas all other months are an average across the whole month. The inflow values are quite variable, corresponding to the observed variation in rainfall, whereas outflow values are very consistent and mostly below 2.0 mm/day, indicating the very high retention capabilities of this partially-infiltrating bioretention system.

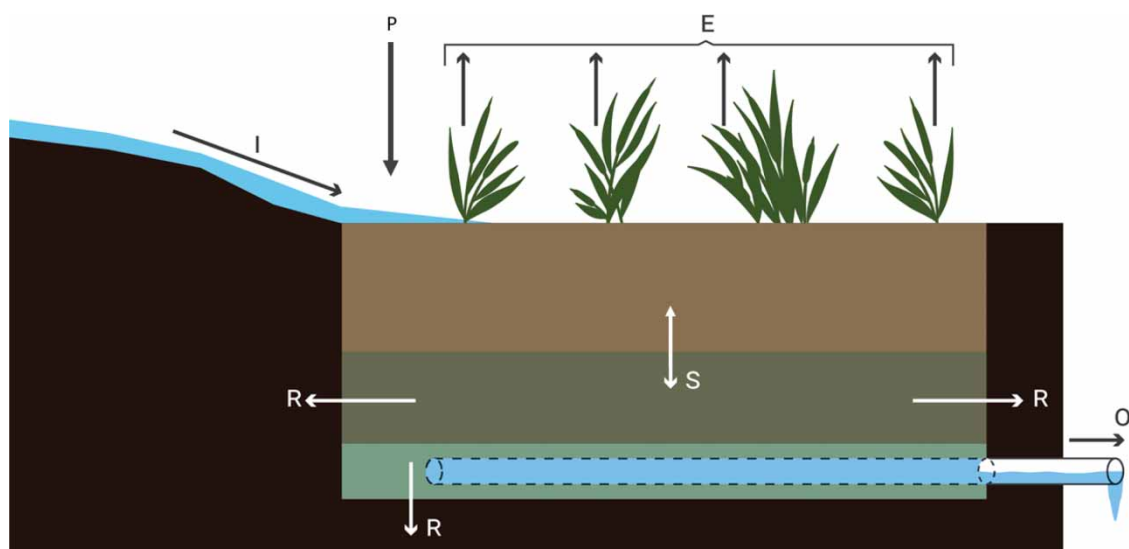


Figure 3 | Schematic of bioretention system water balance.

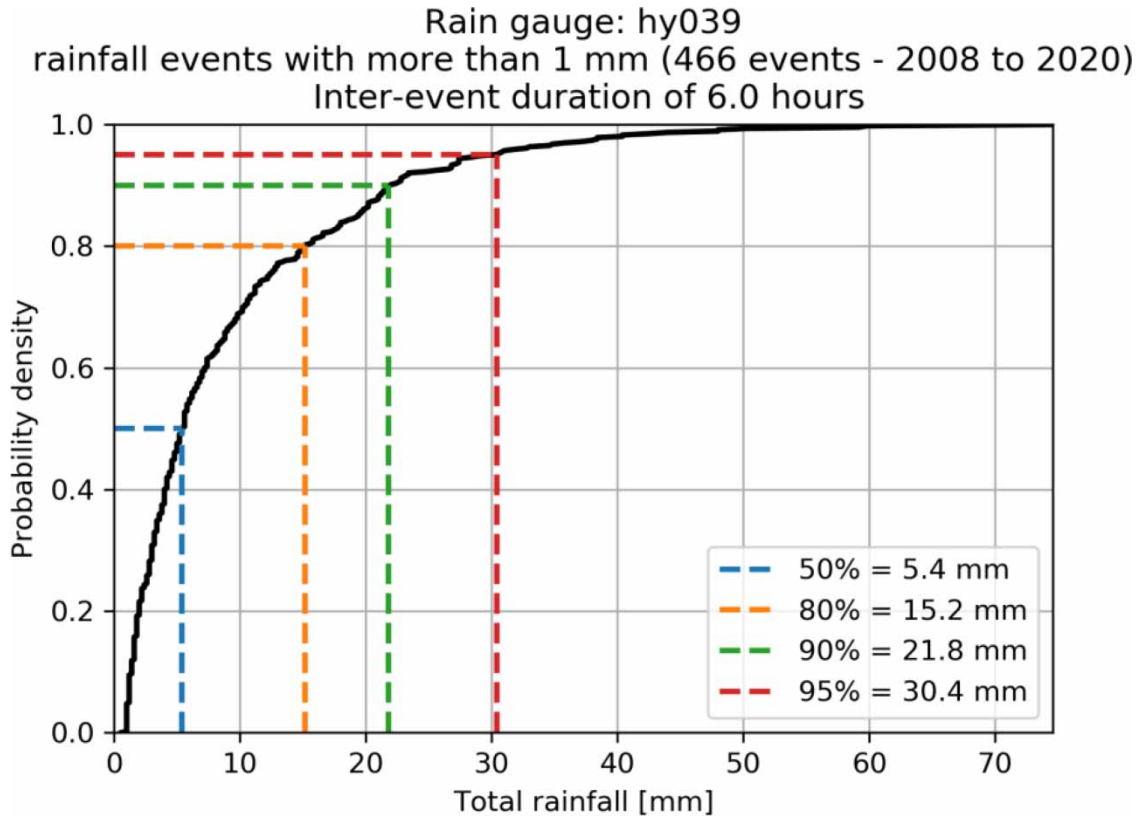


Figure 4 | CDF curves for rainfall events greater than 1 mm, by rainfall depth.

Table 2 | Mean daily inflow, outflow, and retention

Monitoring Period	Average of Inflow (mm/day)	Standard deviation of Inflow (mm/day)	Average of Outflow (mm/day)	Standard deviation of Outflow (mm/day)	Average Retention (mm/day)	Standard deviation Retention (mm/day)
Aug-18	50	41	14	25	36	28
Sep-18	15	11	4	7.8	11	6.2
Oct-18	41	42	2.1	5.5	39	41
Nov-18	69	88	2.1	2.9	67	85
May-19	31	29	0.3	0.4	30	28
Jun-19	17	12	0	0	17	12
Jul-19	20	24	1.1	1.7	19	22
Aug-19	22	21	0.1	0.2	22	21
Sep-19	20	24	0.6	1.4	19	22
Oct-19	52	60	0.5	0.9	51	59
2018	39	41	4.5	11	34	38
2019	28	34	0.4	1	28	34
Full Monitoring Period	31	36	1.7	6.3	30	35

Note: August 2018 and November 2018 were not complete months.

Storage and water content

Water content within the lysimeter remained relatively stable in 2018, varying between 25 and 35%. In 2019, this pattern continued, with the exception of a very dry period in June–July, where water content dropped to 15–20% in all three sensors. The water content remained between 20–30% for July and August after some rainfall events

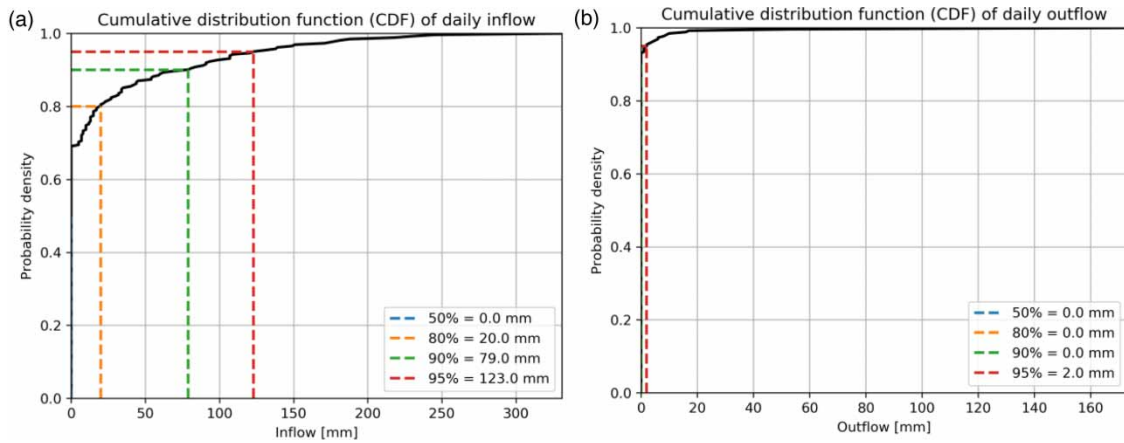


Figure 5 | CDF curves for daily inflow (a) and daily outflow (b).

but did not recover to the average 25–35% water content until October. Water content with rainfall and evapotranspiration are shown in Figure 6, and includes water content in the soil at the nearby weather station, HY039, to compare to a soil that does not receive stormwater inputs. The HY039 water content follows the same pattern of responsiveness to precipitation inputs as the water content in the bioretention system. However, the water

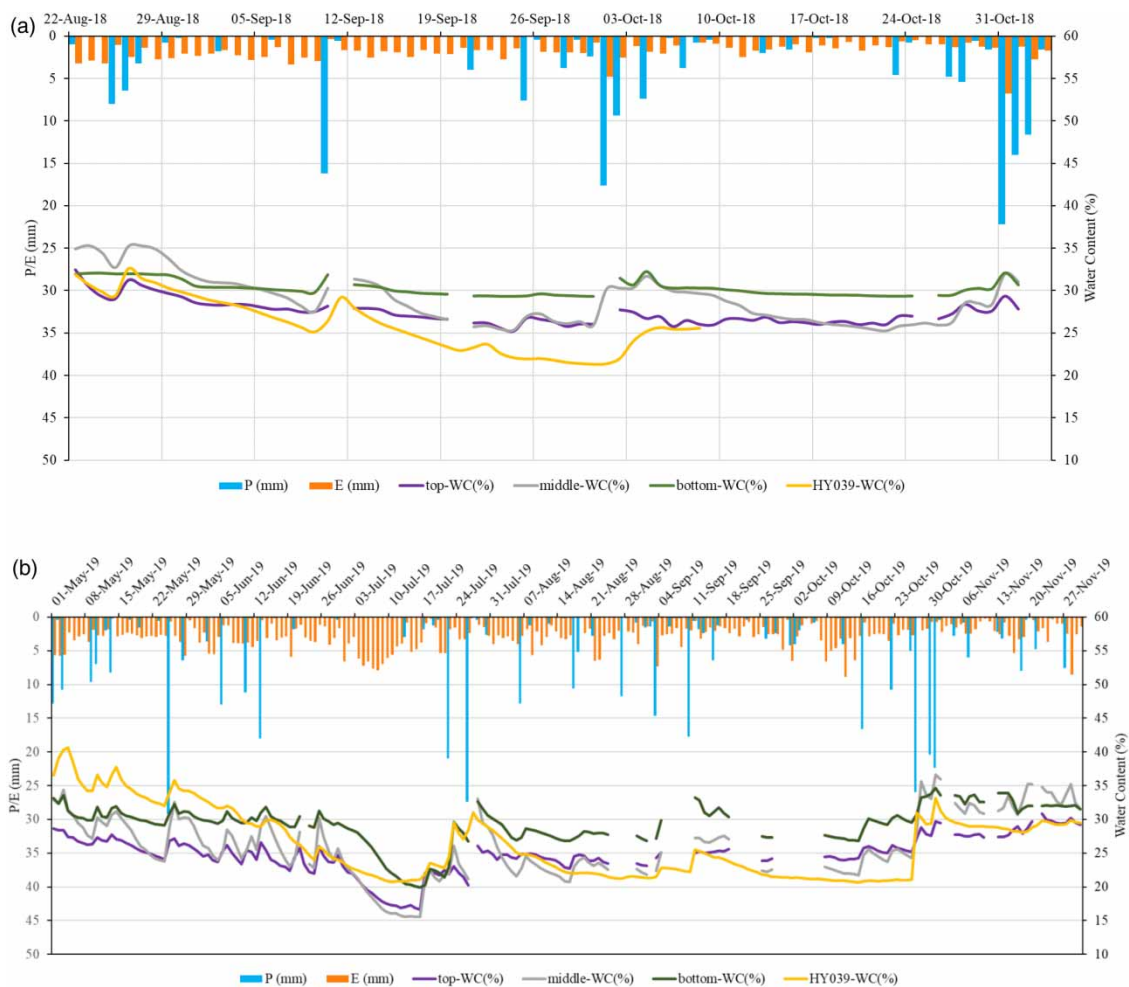


Figure 6 | Precipitation (*P*), evapotranspiration (*E*), and VWC in 2018 (a) and 2019 (b). WC was measured in the top 10 cm (top-WC %), middle 10–20 cm (middle-WC %), and in the bottom 10 cm (bottom-WC %) of the lysimeter tank depth of 30 cm, as well as at the nearby weather station (HY039-WC %).

content at HY039 was notably higher in the spring (May) and lower in the fall (September–October), indicating that the stormwater inputs into the bioretention may be raising water content in the soil.

Evapotranspiration

The average and median daily evapotranspiration rate for the monitoring period are 2.3 and 2.1 mm/day, respectively, and ranged from 0 to 7.5 mm/day. The average daily evapotranspiration rate (mm/day) by month is shown in Table 3, and the CDF for daily evapotranspiration is shown in Figure 7. The lowest evapotranspiration rates were in the fall of 2018, which were even lower than the fall of 2019, though it is unclear which climatic factors drove this difference. The active growing season for *Rudbeckia hirta* is June–August, during which the average daily evapotranspiration increased to an average of 2.9 mm/day. Evapotranspiration increases in the warmer months, even more so during the growing season, and decreases in the cooler and wetter fall season. The majority (80%) of days with evapotranspiration were less than or equal to 3.4 mm.

These results are similar to the evapotranspiration calculated at the HY039 weather station, where daily evapotranspiration for April–November was 2.3 mm/day, and June–August was 3.4 mm/day (Delidjakova *et al.* 2014). This system had lower overall evapotranspiration than an irrigated green roof (another type of the GSI) in the same climate zone, which had an average annual evapotranspiration of 4 mm/day and a peak monthly average evapotranspiration of 5.8 mm/day in July (Jahanfar *et al.* 2018).

Water balance

There were 60 wet events during the monitoring period and 53 dry events during the monitoring period. The average number of days during dry events was 3.8. When combining wet and dry events into a single water balance event, the average number of days per water balance event was 4.1.

The water balance as a portion of inflow is shown in Figure 8. Recharge was the largest net loss of runoff (88%), with evapotranspiration the next largest at 6% of the inflow. Storage was relatively unchanged during the monitoring period, with only a 1% change in storage.

Water balance by small, medium, and large events

The summary of water balance as a percentage of inflow is shown in Figure 9 for the three different categories (small, medium, and large events). Statistically significant differences were found for evapotranspiration as a portion of inflow between the small, medium, and large event sizes (p -value 8.5×10^{-6}). Similarly, outflow and recharge as a portion of inflow were significantly different between the small, medium, and large event sizes (p -values of 1.2×10^{-2} and 2.9×10^{-4} , respectively). As rainfall amounts decrease, the proportion of water that leaves the bioretention system as outflow decreases while the proportion that leaves as evaporation increases.

Table 3 | Average daily evapotranspiration rates

Monitoring period	Average ET (mm/day)	Standard deviation ET (mm/day)
Aug-18	1.6	0.7
Sep-18	1.7	0.5
Oct-18	1.8	1.3
Nov-18	0.8	0.2
May-19	2.9	1.2
Jun-19	3.6	0.9
Jul-19	2.5	1.4
Aug-19	2.1	1.3
Sep-19	2.6	2.1
Oct-19	2.1	1.4
Growing season	2.5	1.3
2018	1.7	1
2019	2.6	1.4
Full monitoring period	2.3	1.4

Note: August 2018 and November 2018 were not complete months.

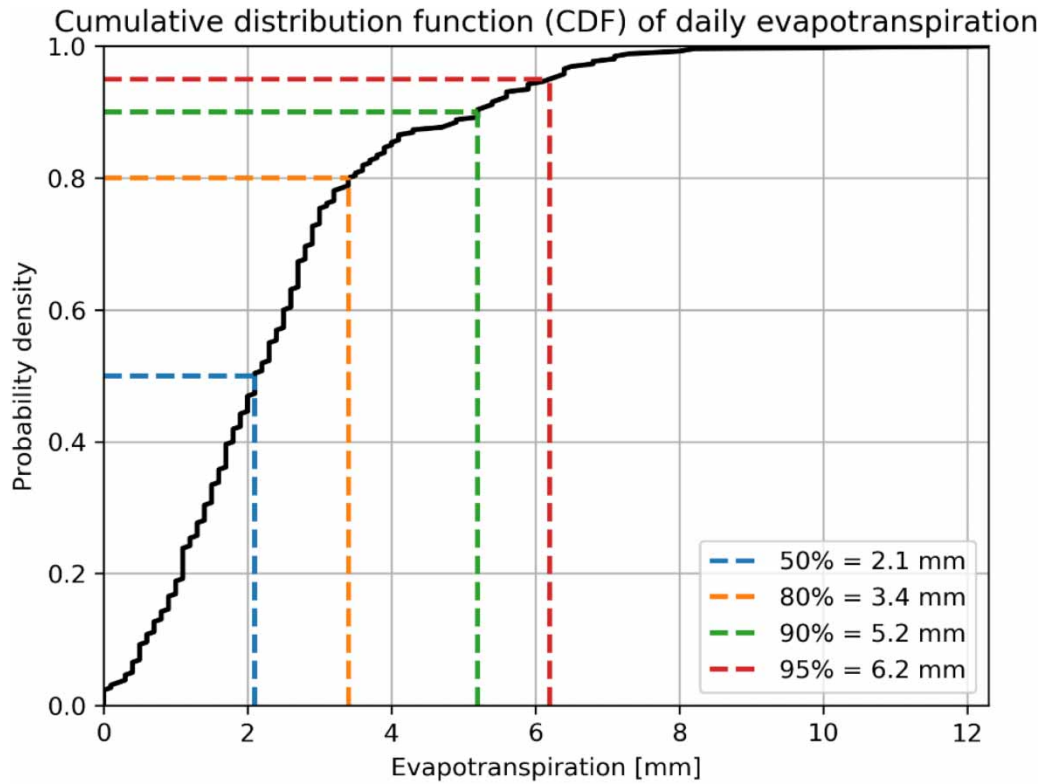


Figure 7 | CDF of daily evaporation.

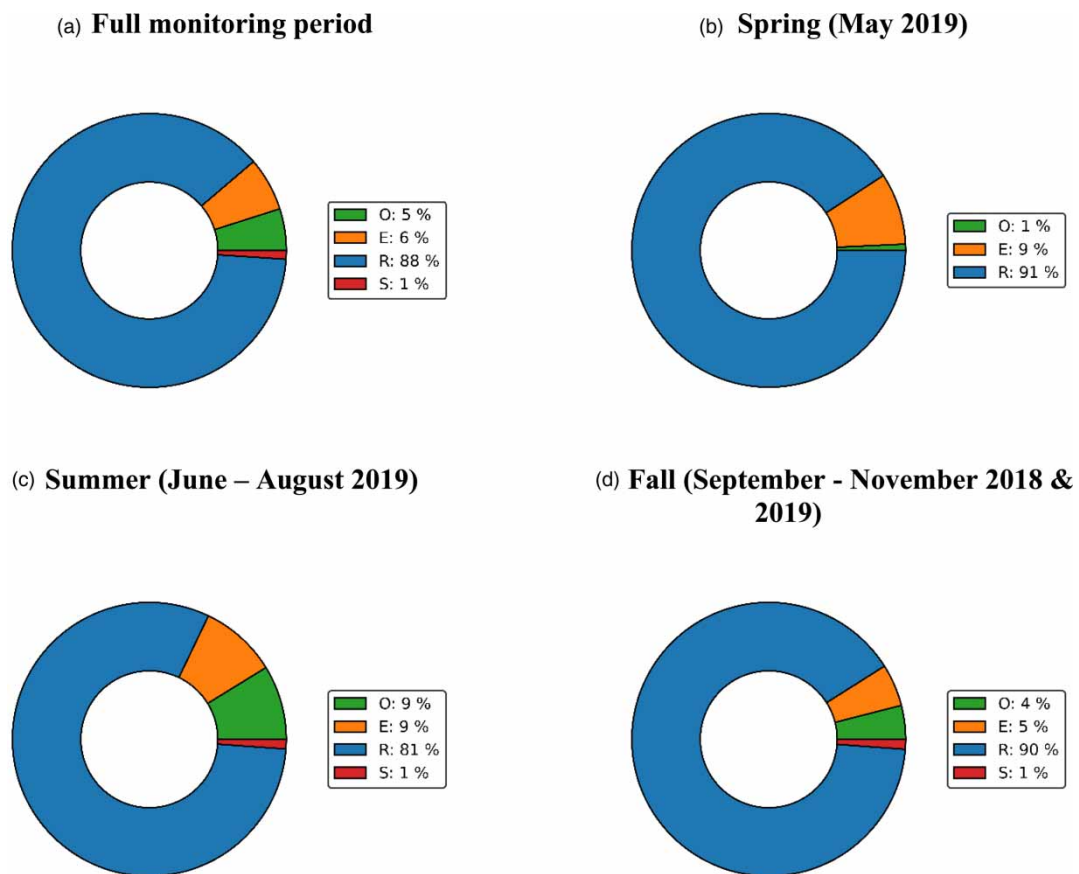


Figure 8 | Water balance of outflow (*O*), evapotranspiration (*E*), recharge (*R*), and storage (*S*) as portion of inflow. Storage not shown in (b) as storage was 0%.

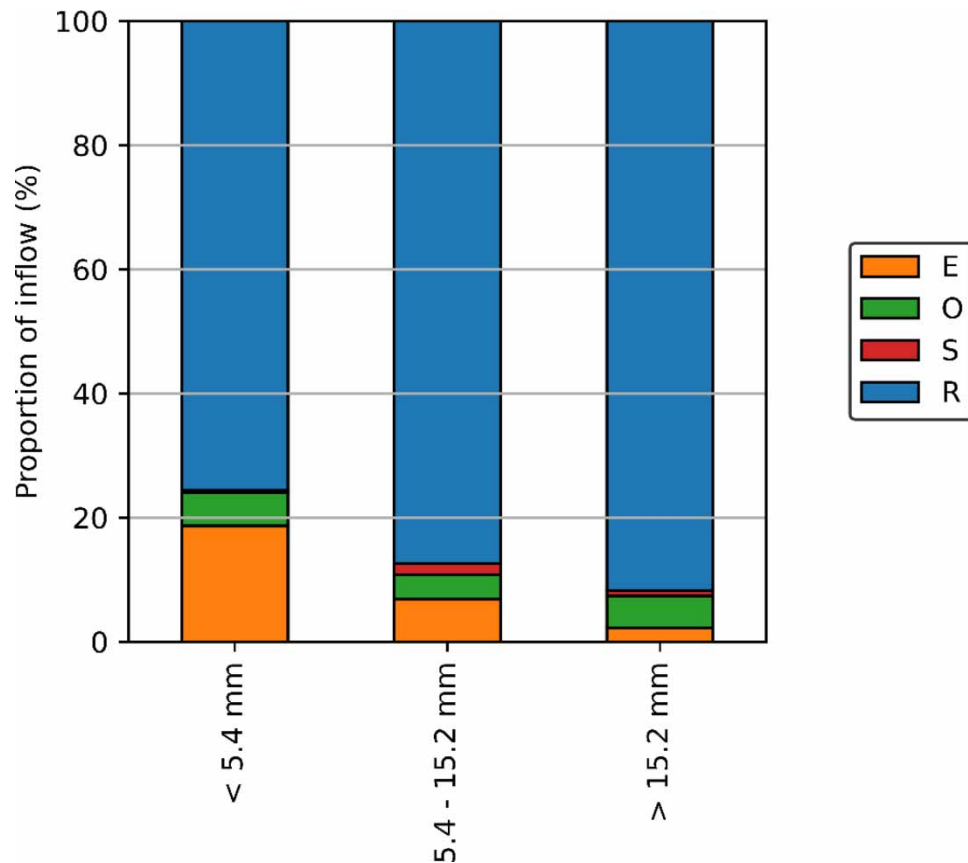


Figure 9 | Water balance for events as a portion of inflow, for small (<5.4 mm), medium (between 5.4 and 15.2 mm), and large (>15.2 mm) events. Water balance components: *E*, evapotranspiration; *O*, outflow; *S*, storage; *R*, recharge.

Figure 10 is a sunburst diagram of the water balance, which shows the water balance portions of inflow multiplied by the portion of annual events in each event-size range. Small events (<5.4 mm) make up 50% of events, medium events (5.4–15.2 mm) make up 30% of events, and large events (\geq 15.2 mm) make up 20% of events for this region. For the most frequently occurring events (small events), evapotranspiration is a large part of the water balance at 19%.

Water balance for large events (\geq 15.2 mm)

During large events in excess of 15.2 mm, most water was returned to groundwater via recharge (92%). Outflow was greater than evapotranspiration, constituting 5% of inflow, and evapotranspiration 2%. Each event over 15.2 mm (14 events) and its water balance breakdown as a portion of inflow is shown in Figure 11. Storage was an average of 1% of the water balance for large events. Storage could be either positive or negative since the period of the water balance was quite short (an average of 3.3 days for large events), representing either water addition to the system (positive storage) or water loss (negative storage). Outflow from the bioretention system occurred for 64% (9/14) of these large events. There were no overflow events (events above the capacity of the bioretention system, which would have backed up into the parking lot), even for the largest events.

The largest event (rainfall depth of 38 mm) was on August 21, 2018 had the largest outflow, representing 46% of inflow, exceeding all other events by an order of magnitude. The remaining large events were between 15.8 and 38 mm, with an average of 23.1 mm.

Water balance for medium-size events (\geq 5.4 and <15.2 mm)

For events in the medium rainfall size range, recharge continues to make up the largest portion of inflow (87%). Evapotranspiration exceeds outflow as a portion of inflow (on average 7 and 4%, respectively). There were 15 medium-sized events during the monitoring periods, ranging from 6.0 to 10.2 mm, with an average event size of 14.4 mm. Figure 12 shows the water balance for each event as a percentage of inflow amount. The average

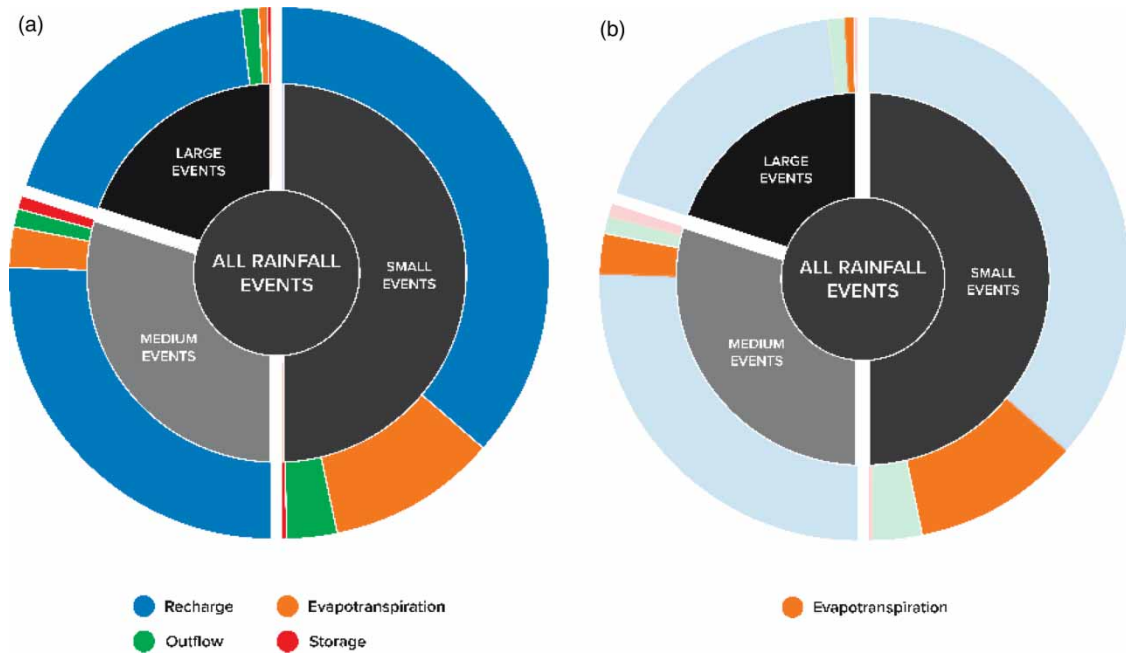


Figure 10 | Sunburst diagram of water balance for small, medium, and large events, where the size of events is relative to their frequency of occurrence (e.g., small events 50%). (a) is the full water balance per event and (b) has evapotranspiration highlighted.

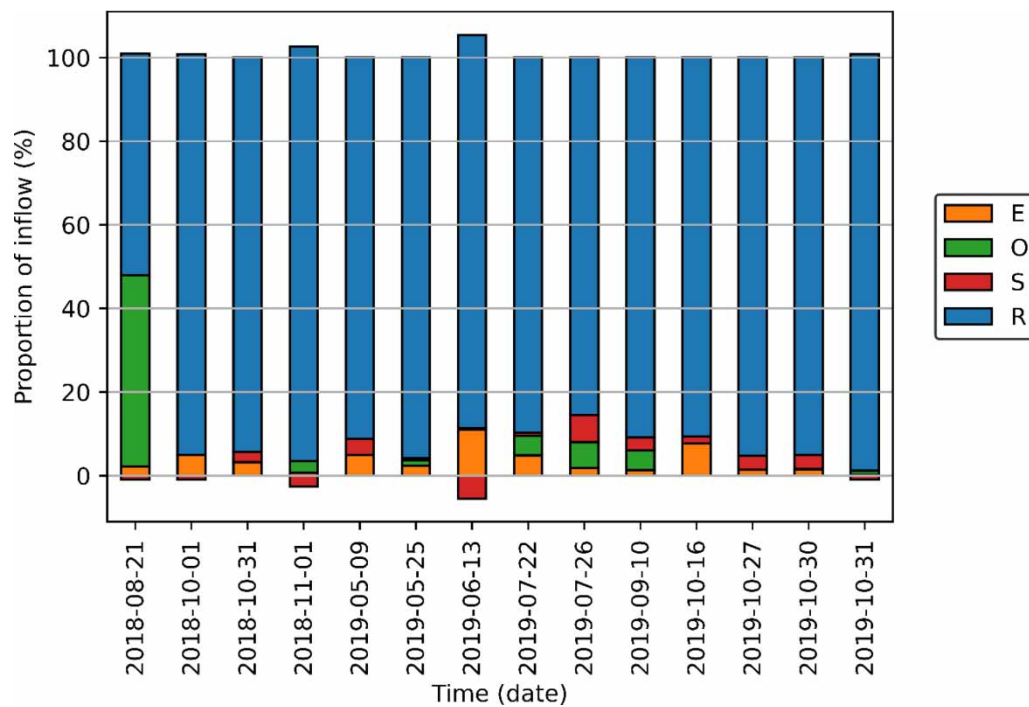


Figure 11 | Water balance for events ≥ 15.2 mm, as percentage of inflow. Water balance components: E, evapotranspiration; O, outflow; S, storage; R, recharge.

duration for a water balance event in the medium-size range was 4.8 days. Three events had large (almost 10–15%) negative storage, resulting from losing water to evapotranspiration during prolonged dry periods. Only 40% of medium-sized events (6/15) resulted in some outflow from the bioretention system, with 60% of medium-sized events were completely retained.

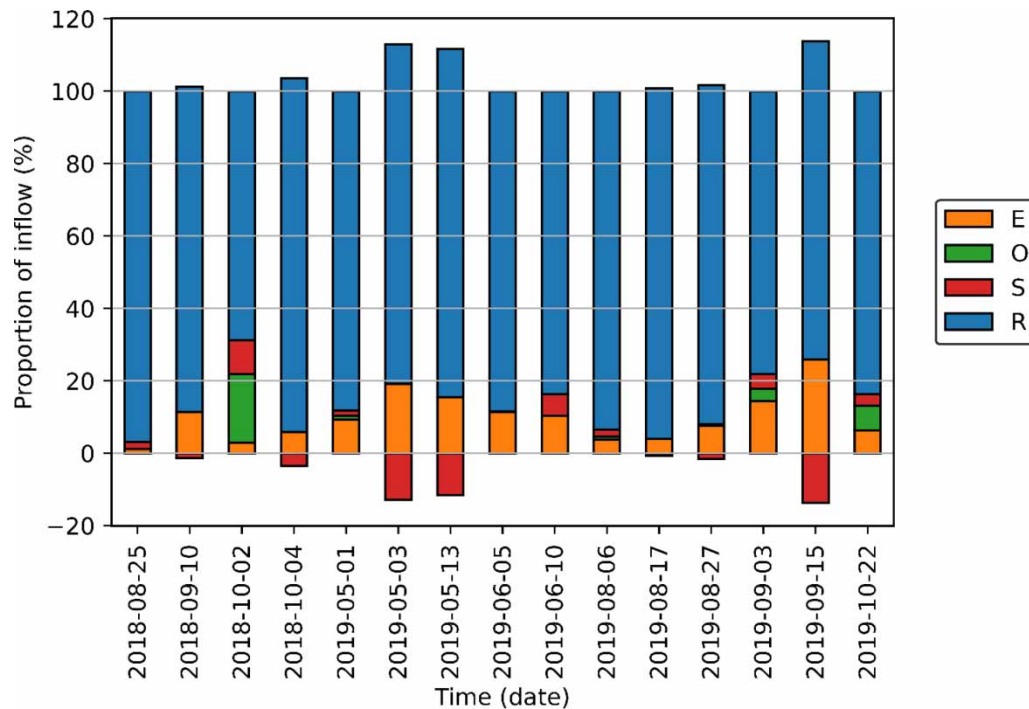


Figure 12 | Water balance for events between 5.4 and 15.2 mm, as percentage of inflow. Water balance components: *E*, evapotranspiration; *O*, outflow; *S*, storage; *R*, recharge.

Water balance for small events (<5.4 mm)

For small rainfall events, only 13% of events (4/31) had outflow at the underdrain. The four events with outflow were all in the fall (three in September 2018 and one in October 2018), which is typically a wetter season with lower evapotranspiration. On average, outflow was only 5% of the total water balance for small events, while evapotranspiration was 19% of inflow and recharge was 76% of inflow. The average duration for a small water balance event was 4.7 days. Storage and recharge were often negative during small events, representing water loss from the system during an extended dry period and that the plants likely pulled water from the surrounding soils during dry events.

Figure 13 shows the water balance for each small event as a percentage of the inflow amount. June 20 to July 10, 2019, was an extended dry period following a small rain event (1.9 mm on June 19, 2019). This event is not

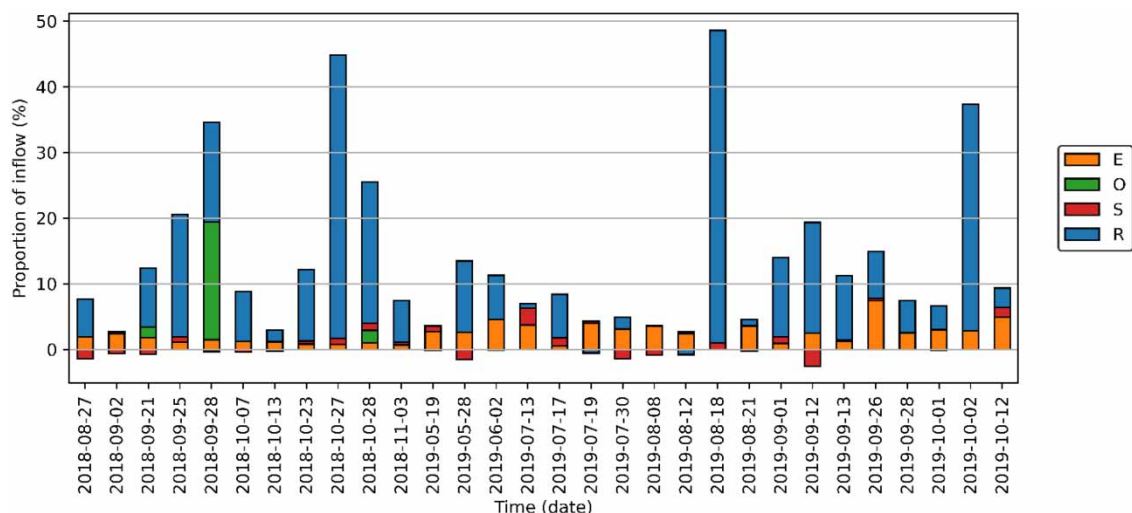


Figure 13 | Water balance for events <5.4 mm, as a percentage of inflow. This figure excludes the water balance event beginning on June 19, 2019. Water balance components: *E*, evapotranspiration; *O*, outflow; *S*, storage; *R*, recharge.

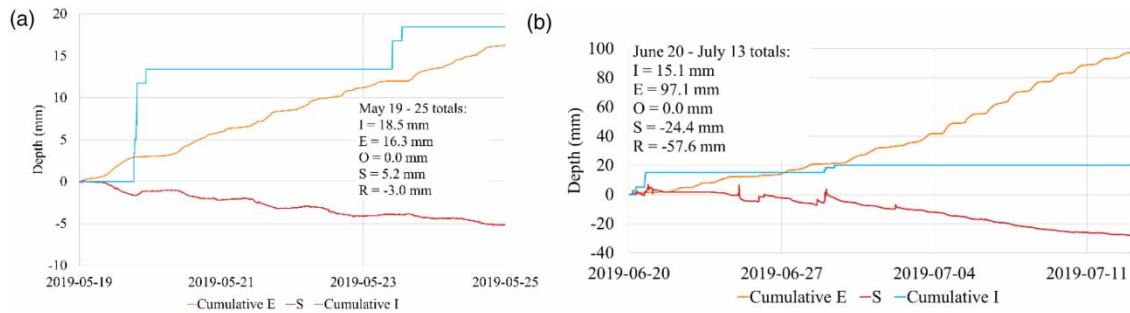


Figure 14 | Cumulative water balance for (a) May 19–25, 2019 and (b) extended dry period of June 20–July 13, 2019. Water balance components: *E*, evapotranspiration; *O*, outflow; *S*, storage; *R*, recharge. Precipitation on the bioretention system is not shown.

shown in Figure 13 and is excluded from summary statistics, as recharge as a portion of inflow was more than –200%, and this skewed the figure and was a large data outlier.

Sub-daily cumulative water balances for two small events, May 19, 2019, with a rainfall depth of 1 mm and June 20, 2019, with a rainfall depth of 1.2 mm, are shown in Figure 14(a). These examples illustrate that during extended dry periods following small rainfalls, evapotranspiration can balance (Figure 14(a)) or far exceeded (Figure 14(b)) inflow. Negative storage and recharge water balance values than occur as the bioretention system lose water to evapotranspiration and has to pull from the surrounding subsurface soil–water system.

DISCUSSION

Performance of the bioretention system

This bioretention system retained a large amount of stormwater runoff (83% of events are completely retained, and the average volume reduction across all events is 97%), preventing it from remaining surface water and returning it to infiltration and evapotranspiration instead. Recharge is the dominant component of water balance, even during large events (recharge is 92% of inflow for large events and 88% of inflow for all events). Outflow from this system is minimal because the valve on the underdrain restricts outflow, which forces increased exfiltration from sidewalls. Soil hydraulic conductivity can occur laterally as well as vertically, with several studies showing that soils can have increased hydraulic conductivity in the horizontal direction compared to the vertical direction (Bathke & Cassel 1991; Chen 2000; Santos & Esquivel 2018). The rectangular shape of the bioretention system results in a significant sidewall area (approximately 8.4 m²), allowing for significant recharge via the sidewalls in addition to the bottom of the bioretention system.

Impact of the rainfall event size on the water balance

The water balance, as a portion of inflow, was different for outflow, recharge and evapotranspiration between the three different rainfall event-size categories. As a portion of inflow, the evapotranspiration for small events was significantly larger than for the complete water balance (19 vs. 6%, p -value 10^{-10}). Outflow and evapotranspiration make up similar proportions of inflow (5 and 6%, respectively) when considering the whole water balance. Evapotranspiration is a significantly larger proportion of the water balance when considering small and medium events only. This shows the importance of evaluating the water balance and performance of the bioretention system using the events for which the system was designed, and not an annual water balance containing all events for which the system was not designed.

Other studies on evapotranspiration in the GSI have included all events in their analysis, even relatively large events, and so the water balance becomes skewed towards those larger events. For example, a previous study at the same site used the Bowen Ratio Energy Balance to model evapotranspiration between storm events and found that evapotranspiration was 12% of inflow (Sustainable Technologies Evaluation Program 2015), and this included all storm events monitored between May and October in 2013 and 2014. In other studies where inflow and outflow were monitored and evapotranspiration was modelled, and including large and small events in the analysis, evapotranspiration as a portion of inflow ranged from 2 to 4% for systems with a drainage area to bioretention area of between 20:1 and 25:1 (Muthanna *et al.* 2008; Strauch *et al.* 2015; Bonneau

et al. 2020). The design rainfall amount used to size the GSI should be based on local rainfall statistics, and performance should be evaluated based on the most frequently recurring events.

The significant role of evapotranspiration

Evapotranspiration was a large part of the water balance, at 19%, for 50% of rainfall events for the system. The large inflow depths (ranging from 0.7 to 188 mm per day) relative to the evapotranspiration depths (ranging from 0 to 7.5 mm per day) can explain why engineers have typically ignored this as a portion of the water balance. However, for some small events, stormwater retention targets may be achieved entirely or almost entirely through evapotranspiration. For example, on May 19, 2019, inflow was 18.5 mm (precipitation of 2.2 mm), and evapotranspiration over the next 6 dry days was a total of 16.3 mm (2.7 mm/day) (see [Figure 12\(a\)](#)). Similarly, in [Hess et al. \(2019\)](#), the dry period between storm events had an average evapotranspiration of 16 mm in a conventional system with an underdrain, and 30 mm in a system with internal water storage and an elevated underdrain.

Current guidance on bioretention design sizes the systems based on the rate at which water leaves the system through exfiltration and outflow only (*e.g.*, CVC & TRCA 2010; [Healthy Waterways Initiative 2014](#); [CIRIA 2015](#); [New York State Department of Environmental Conservation 2015](#)), and does not account for water leaving the system through evapotranspiration. If up to 19% of the design volume of stormwater can be lost over subsequent dry days through evapotranspiration, then using sizing methods based on only losing water to recharge/outflow will result in systems that are larger than necessary. It could be possible to design bioretention systems with a smaller footprint if accounting for water lost to evapotranspiration.

Evapotranspiration for bioretention ranges from 0 to 7.5 mm/day, with an average of 2.3 mm/day overall at 2.9 mm/day in the growing season, and 80% of days less than or equal to 3.4 mm/day. We hypothesize that evapotranspiration rates were able to remain so high because stormwater runoff is concentrated into a small area and keeps the soil moisture content higher than just via direct rainfall. Evapotranspiration increases with vegetation growth, soil moisture content, temperature, and it decreases at high relative humidity ([Chin 2013a](#)). In this study, the moisture content is maintained at fairly consistent levels throughout the monitoring period (see [Figure 6](#)), which is likely due to the continuous large additions of water via stormwater runoff. Indeed, the soil water content in the bioretention system was higher in the fall than the soil water content at the fallow field, indicating that the additional inflow water from stormwater may allow for increased water retention after the dry periods in summer. The only period when soil moisture decreases is during an extended dry period in the middle of summer 2019 (see [Figure 6\(b\)](#)), though this did not lead to plant death in the bioretention system because all species were selected for their drought-tolerance. Given the variability observed in daily evapotranspiration rates we recommend that hydrologic modellers use evapotranspiration rates of 2.1–3.4 mm/day for summer bioretention conditions, and use values of 1–2 mm/day for winter, spring and fall bioretention conditions for systems in climates similar to this study (*i.e.*, Southern Ontario).

Climate change and water balance

Engineers and researchers need to consider whether the GSI will need to be adapted to changing climate conditions. It is helpful to consider which climate change impacts are likely to occur in the area where this study was performed and evaluate whether or not climate changes will result in alterations to the water balance.

Mean annual precipitation is very likely to increase in Ontario (Canada) by 5.5–6.6% by 2050 and 5.3–17.3% by 2100 ([Zhang et al. 2019](#)) while summer precipitation is projected to decrease by the end of the 21st century under a high emission scenario ([Zhang et al. 2019](#)). Increased mean annual temperatures, accompanied by more hot summer days, will likely increase evapotranspiration. This increase in evapotranspiration, combined with a decrease in summer precipitation, could decrease inflow, outflow and recharge in favour of evapotranspiration in bioretention systems. In a sense, this could increase the performance of these bioretention systems for which the main goal is to reduce direct outflow for frequent rainfall events. Extended dry and hot periods in summer under climate change conditions could lead to impacts on plants that could also impact hydrology. For example, plants and soils that dry out severely could result in plant death, which reduces soil structure and could cause short-circuiting, which could lead to less retention and increased outflow.

With projected longer growing seasons, shorter snow and ice cover seasons, and an increase in rain-on-snow events ([Lemmen & Bush 2019](#)), it can be expected that bioretention systems like the one in this study will become increasingly solicited in this future climate. This has the opportunity to increase the number of rainfall events that could be treated by the GSI.

With respect to extreme rainfall events, many studies have reported increases in their frequency and intensity under a warmer climate. For example, the 20-year return period precipitation event could become a 6-year return period (or between 3–4 times more frequent) on average at the global scale (Kharin *et al.* 2013; Martel *et al.* 2020). An increase in inflow to bioretention systems during extreme rainfall events will likely increase the amount of outflow (*e.g.*, see the August 21, 2018 event from Figure 11). While bioretention systems are currently not typically designed to retain extreme rainfall events, the decentralized GSI still can provide a reduction in peak flow (Morsy *et al.* 2016; Winston *et al.* 2016; Spraakman *et al.* 2020b). Furthermore, they can certainly be adapted to deal with extreme rainfall better, ultimately playing a more significant role in climate change resilience (McPhillips *et al.* 2020).

Bioretention design in a changing climate

The rainfall amount that bioretention systems are designed to retain is often defaulted to 25 mm, regardless of climate or rainfall frequency analyses. The 90th percentile rainfall amount for this area, from local rainfall statistics, was found to be 21.8 mm. This amount may change in the future due to climate change, though it is uncertain how rainfall frequency will change. We recommend conducting rainfall frequency analyses regularly so that regulators and designers use design standards that best reflect their local climate. Considering the service life of a typical bioretention system of 20–25 years (CVC & TRCA 2010; Gulliver *et al.* 2010), the design rainfall amount may change slightly over the asset's life, perhaps should be re-sized during rehabilitation.

Frequently, designers and engineers in stormwater management will use continuous simulation to show how their systems will function over the long term. Designers should use recent rainfall data when conducting continuous simulations, to ensure that recent climate changes are accounted for. Continuous simulation is also helpful for more accurately predicting the effect of evapotranspiration on the water balance, thereby ensuring that systems are not oversized when considered this additional water loss. We recommend that designers use evapotranspiration when modelling at the continuous scale, and can use the daily evapotranspiration amounts listed in Table 3, if in a similar climate, or obtain daily evapotranspiration rates from local climate or agricultural data sources.

Some aspects of bioretention design may also need to be altered under climate change conditions. For sustaining vegetation under extended dry periods in summer, media should contain more fines (silt and clay) which increases the plant available water in soils. Also, organic matter such as compost additions and/or mulch should be added regularly to bioretention systems to enhance moisture retention. More intense and short rainfalls could be accommodated by energy dissipation at inlets and/or larger inlets and pre-treatment devices at inlets, so that intense events with small overall rainfall depths do not consistently bypass bioretention systems.

CONCLUSION

This study looked to determine if the bioretention systems was retaining the intended rainfall volume, and show how that water balance was divided between infiltration, outflow and evapotranspiration. The bioretention system achieved very high retention (average 31.2 mm/day) and retained 97% of stormwater runoff volumes. We hypothesized that evapotranspiration composes a more significant portion of the water balance for the small events for which GSI systems are designed. In this study, we divided the water balance results into three rainfall event-size ranges: small (<5.4 mm), medium (between 5.4 and 15.2 mm) and large (above 15.2 mm). We found that evapotranspiration accounted for 19% of the water balance for the small and regularly recurring events for which GSI systems are designed. This value was significantly different from the overall water balance evapotranspiration of 6% of the inflow. As evapotranspiration is not often accounted for in the design of bioretention systems, it results in oversizing the systems, hence the very large stormwater runoff reductions achieved at this site.

The impact of vegetation on GSI systems is clearly significant because, without the transpiration component, it would likely result in increased outflows. The selection of soil media and vegetation needs to be appropriate to sustain soil moisture content in the system and to be adaptable to the local climate. In this bioretention system, we argue that the soil moisture content is maintained by a large amount of runoff (due to the size of the drainage area relative to the bioretention area) and that this maintains a consistent level of evapotranspiration that reduces outflow from the system.

It is crucial to evaluate GSI water balance over the rainfall events for which it was designed to see the system's performance within its optimal design parameters. Climate change will shift rainfall patterns, so it is also essential to re-examine rainfall frequency for the local area and refine GSI criteria accordingly.

DATA AVAILABILITY STATEMENT

All relevant data are included in the paper or its Supplementary Information.

CONFLICT OF INTEREST

The authors declare there is no conflict.

REFERENCES

- Bathke, G. R. & Cassel, D. K. 1991 Anisotropic variation of profile characteristics and saturated hydraulic conductivity in an ultisol landscape. *Soil Science Society of America Journal* **55** (2), 333–339. doi:10.2136/sssaj1991.03615995005500020005x.
- Beck, H. E., Zimmermann, N. E., McVicar, T. R., Vergopolan, N., Berg, A. & Wood, E. F. 2018 Present and future Köppen-Geiger climate classification maps at 1-km resolution. *Sci Data* **5**, 180214. doi:10.1038/sdata.2018.214.
- Bonneau, J., Fletcher, T. D., Costelloe, J. F., Poelsma, P. J., James, R. B. & Burns, M. J. 2020 The hydrologic, water quality and flow regime performance of a bioretention basin in Melbourne, Australia. *Urban Water Journal* **17** (4), 303–314. doi:10.1080/1573062x.2020.1769688.
- Chen, X. 2000 Measurement of streambed hydraulic conductivity and its anisotropy. *Environmental Geology* **39** (12), 1317–1324.
- Chin, D. A. 2013a Estimation of evapotranspiration. In: H. Stark, ed. *Water Resources Engineering*, 3rd edn. Pearson Education Inc, Upper Saddle River, New Jersey.
- Chin, D. A. 2013b Fundamentals of Surface-Water Hydrology II: Runoff. In: H. Stark, ed. *Water Resources Engineering*, 3rd edn. Pearson Education Inc, Upper Saddle River, New Jersey.
- CIRIA. 2015 *The SUDS Manual*. CIRIA, London. Retrieved from Dundee, Scotland.
- Corder, G. W. & Foreman, D. I. 2009 *Nonparametric Statistics for Non-Statisticians*. John Wiley & Sons, Hoboken, NJ.
- Credit Valley Conservation, & Toronto and Region Conservation. 2010 *Low Impact Development Stormwater Management Planning and Design Guide*. Credit Valley Conservation, & Toronto and Region Conservation.
- Davis, A. P., Hunt, W. F., Traver, R. G. & Clar, M. L. 2009 Bioretention technology: overview of current practice and future needs. *Journal of Environmental Engineering* **135** (3), 109–117. doi:10.1061/(ASCE)0733-9372(2009)135:3(109).
- Delidjakova, K., Bello, R. & MacMillan, G. 2014 *Measurement of Evapotranspiration Across Different Land Cover Types in the Greater Toronto Area*.
- Denich, C. & Bradford, A. 2010 Estimation of evapotranspiration from bioretention areas using weighing lysimeters. *Journal of Hydrologic Engineering* **15** (6), 522–530. doi:10.1061/(ASCE)HE.1943-5584.0000134.
- Gulliver, J. S., Erickson, A. J. & Weiss, P. T. 2010 *Stormwater Treatment: Assessment and Maintenance*. University of Minnesota, St. Anthony Falls Laboratory, Minneapolis, MN.
- Hannes, M., Wollschlager, U., Schrader, F., Durner, W., Gebler, S., Putz, T., Fank, J., von Unold, G. & Vogel, H.-J. 2015 A comprehensive filtering scheme for high-resolution estimation of the water balance components from high-precision lysimeters. *Hydrology and Earth System Sciences* **19** (8), 3405–3418.
- Harris, C. R., Millman, K. J., van der Walt, S. J., Gommers, R., Virtanen, P., Cournapeau, D. & Oliphant, T. E. 2020 Array programming with NumPy. *Nature* **585** (7825), 357–362. doi:10.1038/s41586-020-2649-2.
- Healthy Waterways Initiative. 2014 *Bioretention Technical Design Guidelines*. Healthy Waterways Ltd, Brisbane.
- Hess, A., Wadzuk, B. & Welker, A. 2017 Evapotranspiration in rain gardens using weighing lysimeters. *Journal of Irrigation and Drainage Engineering* **143** (6), 04017004–04017004. doi:10.1061/(asce)ir.1943-4774.0001157.
- Hess, A., Wadzuk, B. & Welker, A. 2019 Predictive evapotranspiration equations in rain gardens. *Journal of Irrigation and Drainage Engineering* **145** (7), 04019010. doi:10.1061/(ASCE).
- Hunter, J. D. 2007 Matplotlib: a 2D graphics environment. *Computing in Science & Engineering* **9** (3), 90–95. doi:10.1109/MCSE.2007.55.
- Jahanfar, A., Drake, J., Sleep, B. & Gharabaghi, B. 2018 A modified FAO evapotranspiration model for refined water budget analysis for Green Roof systems. *Ecological Engineering* **119**, 45–53. doi:10.1016/j.ecoleng.2018.04.021.
- Kharin, V. V., Zwiers, F. W., Zhang, X. & Wehner, M. 2013 Changes in temperature and precipitation extremes in the CMIP5 ensemble. *Climatic Change* **119** (2), 345–357. doi:10.1007/s10584-013-0705-8.
- Leimgruber, J., Steffelbauer, D. B., Krebs, G., Tscheikner-Gratl, F. & Muschalla, D. 2018 Selecting a series of storm events for a model-based assessment of combined sewer overflows. *Urban Water Journal* **15** (5), 453–460. doi:10.1080/1573062x.2018.1508601.
- Lemmen, D. S. & Bush, E. 2019 *Canada's Change Climate Report*. Government of Canada, Ottawa, ON.
- Li, H., Sharkey, L. J., Hunt, W. F. & Davis, A. P. 2009 Mitigation of impervious surface hydrology using bioretention in north carolina and maryland. *Journal of Hydrologic Engineering(April)* **14** (4), 407–409. doi:10.1061/(ASCE)1084-0699(2009)14:4(407).
- Liu, J., Sample, D., Bell, C. & Guan, Y. 2014 Review and research needs of bioretention used for the treatment of urban stormwater. *Water* **6** (4), 1069–1099. doi:10.3390/w6041069.
- Marsalek, J., Rochfort, Q., Brownlee, B., Mayer, T. & Servos, M. 1999 An exploratory study of urban runoff toxicity. *Water Science and Technology* **39** (12), 33–39. doi:10.2166/wst.1999.0526.

- Martel, J.-L., Mailhot, A. & Brissette, F. 2020 Global and regional projected changes in 100-yr subdaily, daily, and multiday precipitation extremes estimated from three large ensembles of climate simulations. *Journal of Climate* **33** (3), 1089–1103. doi:10.1175/jcli-d-18-0764.1.
- Maryland Department of the Environment. 2009 *Maryland Stormwater Design Manual, Volumes I and II*. Available from: https://mde.maryland.gov/programs/Water/StormwaterManagementProgram/Pages/stormwater_design.aspx.
- McKinney, W. & Pandas Development Team 2021 pandas: powerful Python data analysis toolkit. In *Release 1.2.1*.
- McPhillips, L. E., Matsler, M., Rosenzweig, B. R. & Kim, Y. 2020 What is the role of green stormwater infrastructure in managing extreme precipitation events? *Sustainable and Resilient Infrastructure* **6**, 133–142. doi:10.1080/23789689.2020.1754625.
- Morsy, M. M., Goodall, J. L., Shatnawi, F. M. & Meadows, M. E. 2016 Distributed stormwater controls for flood mitigation within urbanized watersheds: case study of rocky branch watershed in Columbia, south carolina. *Journal of Hydrologic Engineering* **21** (11), 05016025.
- Muthanna, T. M., Viklander, M. & Thorolfsson, S. T. 2008 Seasonal climatic effects on the hydrology of a rain garden. *Hydrological Processes* **22** (11), 1640–1649.
- New York State Department of Environmental Conservation 2015 *Stormwater Management Design Manual*. Albany, NY. Available from: <https://www.dec.ny.gov/chemical/29072.html>. Department of Environmental Conservation, New York State.
- Regehr, A. G. 2019 *Estimation of Evapotranspiration From A Bioretention Facility Using A Lysimeter and Six Predictive Equations*. Master, Applied Science in Engineering, The University of Guelph, Guelph, Ontario.
- Santos, R. A. d. & Esquivel, E. R. 2018 Saturated anisotropic hydraulic conductivity of a compacted lateritic soil. *Journal of Rock Mechanics and Geotechnical Engineering* **10** (5), 986–991. doi:10.1016/j.jrmge.2018.04.005.
- Selbig, W. R. & Balster, N. J. 2010 *Evaluation of Turf-Grass and Prairie-Vegetated Rain Gardens in A Clay and Sand Soil, Madison, Wisconsin, Water Years 2004–08 (2010–5077)*. US Department of the Interior, US Geological Survey.
- Spraakman, S. & Drake, J. 2021 *Bioretention Evapotranspiration*. <https://doi.org/10.4211/hs.e14c468d23274019bc53061c0a42e4aa>.
- Spraakman, S., Rodgers, T. F. M., Monri-Fung, H., Nowicki, A., Diamond, M. L., Passeport, E. & Drake, J. 2020a A need for standardized reporting: a scoping review of bioretention research 2000–2019. *Water* **12** (11), 3122. doi:10.3390/w12113122.
- Spraakman, S., Van Seters, T., Drake, J. & Passeport, E. 2020b How has it changed? A comparative field evaluation of bioretention infiltration and treatment performance post-construction and at maturity. *Ecological Engineering* **158**, 106036. <https://doi.org/10.1016/j.ecoleng.2020.106036>.
- Stewart, R. D., Lee, J. G., Shuster, W. D. & Darner, R. A. 2017 Modelling hydrological response to a fully-monitored urban bioretention cell. *Hydrological Processes* **31** (26), 4626–4638. doi:10.1002/hyp.11386.
- Strauch, K. R., Rus, D. L. & Holm, K. E. 2015 *Water Balance Monitoring for two Bioretention Gardens in Omaha, Nebraska, 2011–14 Scientific Investigations Report 2015–5188*.
- Sustainable Technologies Evaluation Program 2015 *Performance Comparison of Surface and Underground Stormwater Infiltration Practices*. Available from: https://sustainabletechnologies.ca/app/uploads/2016/08/BioVSTrench_TechBrief_July2015.pdf
- Tirpak, R. A., Hathaway, J. M. & Franklin, J. A. 2019 Investigating the hydrologic and water quality performance of trees in bioretention mesocosms. *Journal of Hydrology* **576**, 65–71. doi:10.1016/j.jhydrol.2019.06.043.
- Toronto and Region Conservation Authority. 2020 *Precipitation: Published Data for Kortright (HY039)*.
- UMS gmbH Munchen 2014 *Smart Field Lysimeter User Manual*.
- US EPA 2020 *What is Green Infrastructure?* Available from: <https://www.epa.gov/green-infrastructure/what-green-infrastructure>.
- Virtanen, P., Gommers, R., Oliphant, T. E., Haberland, M., Reddy, T., Cournapeau, D. & SciPy, C. 2020 Scipy 1.0: fundamental algorithms for scientific computing in Python. *Nat Methods* **17** (3), 261–272. doi:10.1038/s41592-019-0686-2.
- Wadzuk, B. M., Hickman, J. M. & Traver, R. G. 2015 Understanding the role of evapotranspiration in bioretention: mesocosm study. *Journal of Sustainable Water in the Built Environment* **1** (2). 04014002-04014001-04014007. doi:10.1061/JSWBAY.0000794.
- Walsh, C. J., Roy, A. H., Feminella, J. W., Cottingham, P. D., Groffman, P. M. & Morgan, R. P. 2005 The urban stream syndrome: current knowledge and the search for a cure. *Journal of the North American Benthological Society* **24** (3), 706–723. doi:10.1899/04-028.1.
- Winston, R. J., Dorsey, J. D. & Hunt, W. F. 2016 Quantifying volume reduction and peak flow mitigation for three bioretention cells in clay soils in northeast ohio. *Science of the Total Environment* **553**, 83–95. doi:10.1016/j.scitotenv.2016.02.081.
- Zhang, X., Flato, G., Kirchmeier-Young, M., Vincent, L., Wan, H., Wang, X., Kharin, V. V., 2019 Temperature and Precipitation Across Canada. In: *Canada's Changing Climate Report* (Bush, E. & Lemmen, D. S. eds). Government of Canada, Ottawa, Canada.

First received 8 February 2022; accepted in revised form 19 July 2022. Available online 3 August 2022